analyzer," *IEEE Trans. Microwave Theory Tech.*, vol. MTT-25, pp. 1086–1091, Dec. 1977.

✤

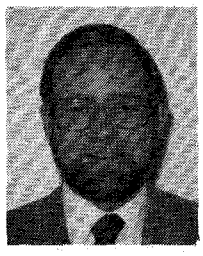

Gordon P. Riblet (M'73) was born in Boston, MA, on December 12, 1943. He received the M.S. and Ph.D. degrees in physics from the University of Pennsylvania, Philadelphia, PA, in 1966 and 1970, respectively.

From 1970 to 1972 he was employed as a Research Scientist at the University of Cologne, Cologne, Germany, performing research in solid-state physics. Since 1972 he has been employed as a Research Scientist at Microwave Development Laboratories, Natick, MA, working in the areas of ferrite devices and computerized test measurements.

E. R. Bertil Hansson was born in Strömstad, Sweden, on June 20, 1945. He received the M.Sc. and Ph.D. degrees in electrical engineering from Chalmers University of Technology, Gothenburg, Sweden, in 1970 and 1979, respectively.

From 1970 to 1980 he was a Research Assistant at the Division of Network Theory, Chalmers University of Technology. His field of interest at that time was planar microwave ferrite components, in particular, junction circulators and phase shifters. In 1979 he received a scholarship from the Sweden—America Foundation for postgraduate studies in the United States, and was with Microwave Development Laboratories, Inc., Natick, MA, from 1980 to 1982. At M.D.L. he was engaged in theoretical and experimental investigations in the fields of computerized test measurements and planar microwave structures. At present he is in Sweden with the Division of Network Theory, Chalmers University of Technology, engaged in a postgraduate research and teaching program.

Efficient Eigenmode Analysis for Planar Transmission Lines

ABDELMEGID KAMAL SAAD, STUDENT MEMBER, IEEE, AND KLAUS SCHÜNEMANN, MEMBER, IEEE

Abstract—**A unified analysis for planar transmission lines is performed using the mode-matching technique. Exploiting the fact that the thickness of the metal coating (fins or strips) is usually very small in comparison to all other dimensions, the characteristic equations are formulated in a way which preserves the physical meaning of their individual terms. Thus, simplifications of far-reaching consequences can be introduced for all eigenmodes showing a cutoff frequency. It is shown in particular that the higher order modes can be derived approximately from the fundamental mode. Moreover, the dispersion relation of fin-lines can be given by a simple expression because the equivalent dielectric constant linearly depends on frequency. Both steps reduce the computer time by about two orders of magnitude in comparison to the spectral-domain method.**

I. Introduction

NUMEROUS PAPERS have appeared dealing with a rigorous solution of the dispersion problem of various planar transmission lines. Highly sophisticated techniques have been developed and applied, one of the most favorable being the spectral-domain method in conjunction with Ritz–Galerkin's method. Two references may stand for many investigations: [1], [2]. Common to all of these works is a time-consuming evaluation of the final relations. Hence, there are but few papers dealing with an application of the eigenmode analysis to circuit problems. This contribution deals with an approximate and efficient analysis of planar transmission lines and its application to fin-lines. Using the mode-matching technique, the final equations are formulated in a way which allows introducing some essential simplifications. The main difference to existing methods is a reduction in computer time of about two orders of magnitude. Hence, the analysis should be well suited for a computer-aided design of microwave planar circuits.

Manuscript received March 10, 1982; revised June 1, 1982. This work was supported by the Deutsche Forschungsgemeinschaft.

The authors are with the Institut für Hochfrequenztechnik, Technische Universität Braunschweig, Postfach 3329, D-3300 Braunschweig, West Germany.

II. Analysis

The structure which has been analyzed consists of an arbitrary number of metallic strips which are deposited on either side of a dielectric substrate. This planar circuit may be mounted either in the *H*-plane or in the *E*-plane of a rectangular box. Hence, the structure can be specialized to represent a microstrip line, coupled striplines, a slot line, a coplanar line, a microstrip line with tuning septums, a bilateral, unilateral, or antipodal fin-line, and a multislot fin-line. For explaining the calculation procedure, the cross section of the latter is shown in Fig. 1. The metallic strips are assumed to have finite thickness. This eliminates, on one hand, the existence of field singularities due to an edge condition while it is furthermore realistic at frequencies in the upper millimeter-wave range [3].

The eigenmode analysis starts with the well-known

0018-9480/82/1200-2125$00.75 ©1982 IEEE

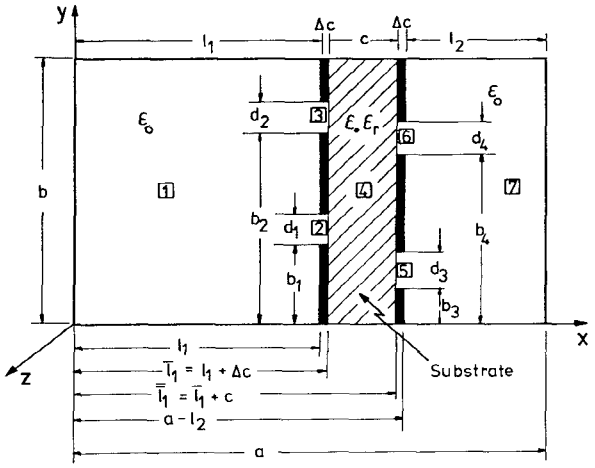

Fig. 1. Cross section of a general planar transmission line.

mode-matching method, which shows some important advantages over other methods: its final equations can be interpreted physically. This allows simplifications of great consequences as will be shown below. Moreover, the method can also directly be applied at the cutoff frequency. An inherent disadvantage is, however, the poor convergence of the solutions. It was the main task of our investigations to remove this restriction.

The cross section of the shielded planar structure of Fig. 1 is divided into 7 regions with 8 boundaries separating these regions from one another. Due to the dielectric substrate, the field is hybrid and can be calculated from 2 scalar potential functions. In region 1 one has, e.g.,

$$\psi_1^H = \sum_{p=0}^{\infty} A_p \cdot \cos(k_{xp}x) \cdot \cos(k_{yp}y) \cdot \exp(-Jk_z z)$$

$$\psi_1^E = \sum_{p=1}^{\infty} \bar{A}_p \cdot \sin(k_{xp}x) \cdot \sin(k_{yp}y) \cdot \exp(-Jk_z z). \quad (1)$$

In the following we will still need the potentials in region 7. They are of course similar to (1) but with amplitudes A_p, $\bar{A}_p$ replaced by G_p, $\bar{G}_p$. The wavenumbers in the x- and y-directions are related via

$$-k_z^2 + k^2 = k_{cmn}^2 = k_{xp}^2 + k_{yp}^2$$
$$-k_z^2 + \epsilon_r k^2 = \bar{k}_{cmn}^2 = \bar{k}_{xp}^2 + k_{yp}^2. \quad (2)$$

Furthermore, $k_{yp} = p\pi/b$, and k means free-space wavenumbers. The second of the separation relations is valid in region 4.

The total field is calculated by a superposition of a TE-term (ψ^H) with a TM-term (ψ^E). One obtains, e.g., in region 1

$$E_{y1} = \sum_{p=0}^{\infty} \left[\frac{A_p}{Y_p} + \frac{\bar{A}_p}{\bar{Y}_p} \cdot (1 - \epsilon_p) \right] \cdot \sin(k_{xp}x) \cdot \cos(k_{yp}y)$$

where

$$Y_p = -\frac{k_{cmn}^2}{J\omega\mu_0 k_{xp}}, \quad \bar{Y}_p = -\frac{k_{cmn}^2}{Jk_{yp}k_z\eta_0^2}, \text{ and } \eta_0^2 = \frac{\mu_0}{\epsilon_0} \quad (3)$$

with $\epsilon_p = 1$ for $p = 0$, and $\epsilon_p = 0$ otherwise. The next step is to match the tangential field components at the various interfaces. Thus, the y-dependence is eliminated due to orthogonality. We will now utilize that the metallization is usually very thin in comparison to all other dimensions. For $\Delta c/a \ll 1$ we can set $\sin(k_x\Delta c) = k_x\Delta c$ and $\cos(k_x\Delta c) = 1$. It is then possible to eliminate the amplitudes of the fields in the slot regions and in the dielectric region which can be explicitly related to the amplitudes of the fields in regions 1 and 7. This is valid for any number of slots or for any number of strips on a dielectric substrate. (The structure of Fig. 1 may also be interpreted as a general strip-line configuration being mounted in the H-plane of the rectangular waveguide.) Thus, one finally arrives at the homogeneous system of equations

$$f(t) = \sum_{p=0}^{\infty} X_p^{(1)} \cdot F_1(t,p), \quad g(t) = \sum_{p=0}^{\infty} X_p^{(2)} \cdot F_2(t,p),$$
$$t = 0, 1 \cdots \infty, \text{ HE-modes}$$
$$\bar{f}(t) = \sum_{p=1}^{\infty} \bar{X}_p^{(1)} \cdot \bar{F}_1(t,p), \quad \bar{g}(t) = \sum_{p=1}^{\infty} \bar{X}_p^{(2)} \cdot \bar{F}_2(t,p),$$
$$t = 1, 2 \cdots \infty, \text{ EH-modes} \quad (4)$$

where $X_p^{(1)}$, $X_p^{(2)}$, $\bar{X}_p^{(1)}$, $\bar{X}_p^{(2)}$, $f(t)$, $g(t)$, $\bar{f}(t)$, and $\bar{g}(t)$ are linear combinations of the amplitudes in regions 1 and 7. Furthermore, they depend on k_{xp}, k_{yp}, k, and dimensions. They are listed in Appendix I. The abbreviations F_1, F_2, $\bar{F}_1$, and $\bar{F}_2$ depend only on dimensions and not on frequency. They are given by

$$F_1(t,p) = \sum_{i,j} \sum_{s=0}^{\infty} f_i^i(t,s) \cdot f_j^i(p,s) \frac{b}{d_j^i} = \sum_{i,j} \sum_{s=0}^{\infty} F_j^{si}$$

$$\bar{F}_1(t,p) = \sum_{i,j} \sum_{s=1}^{\infty} f_i^i(t,s) \cdot f_j^i(p,s) \frac{b}{d_j^i} = \sum_{i,j} \sum_{s=1}^{\infty} F_j^{si} \quad (5)$$

where i denotes the slot number on the left of the substrate and j denotes it on the right. f_i depends on two integers as

$$f_i(p_1, p_2) = \frac{2}{p_1\pi} \cdot \left[\frac{(-1)^{p_2} \cdot \sin(p_1\pi(b_i + d_i)/b) - \sin(p_1\pi \cdot b_i/b)}{1 - (p_2^2/p_1^2)(b^2/d_i^2)} \right],$$
$$\text{for } p_1 d_i \neq p_2 b$$
$$= \frac{d_i}{b} \cos(p_2\pi \cdot b_i/d_i), \; f_i(0,0) = \frac{2d_i}{b},$$
$$\text{for } p_1 d_i = p_2 b. \quad (6)$$

Equation (4) can be explained physically.

1) The first two relations describe the transverse resonance condition of a hybrid HE-mode, the latter two belong to an EH-mode. Setting $\epsilon_r = 1$ yields $E_{1p}^{(1)} = E_{2p}^{(2)} = \bar{H}_{1p}^{(1)} = \bar{H}_{2p}^{(2)} \equiv 0$ (see Appendix I). Then (4) describes purely H-modes (TE-modes) and E-modes (TM-modes), respectively.

2) Matrices $F_1(t,p)$, $F_2(t,p)$, $\bar{F}_1(t,p)$, and $\bar{F}_2(t,p)$ are purely diagonal if the metallization is removed. Hence,

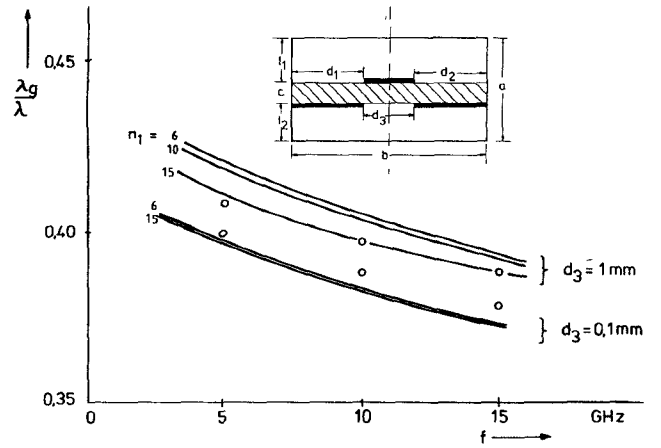

Fig. 2. Guide wavelength versus frequency of a microstrip with tuning septum of width d_3. $a = 24.13$ mm, $b = 12.7$ mm, $l_1 = l_2 = 11.43$ mm, $d_1 = d_2 = 5.715$ mm, $c = 1.27$ mm, $\epsilon_r = 8.875$. λ means free-space wavelength; 0 means results taken from [5]. Parameter is the number of terms in the series expansions.

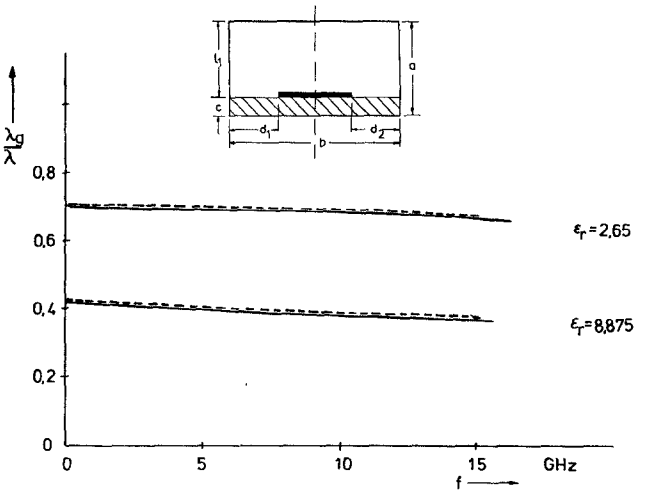

Fig. 3. Guide wavelength of a shielded microstrip versus frequency (solid lines). $a = b = 12.7$ mm, $c = 1.27$ mm, $d_1 = d_2 = 5.715$ mm. Dashed lines denote results taken from [6].

there is no mutual coupling between the expansion terms of the individual regions, which can be treated separately. The transverse resonance condition of the HE_{m0}-modes is then obtained from the first two equations of (4) setting $t = 0$, that of the EH_{m1}-modes from the second couple for $t = 1$, etc. The HE- and EH-modes change into the H- and E-modes of rectangular waveguides for $\epsilon_r = 1$.

3) The structure of the matrices (5) suggests how the general case of more than two slots on either side of the substrate is to be treated. Then the maximum summation indices for i and j have only to be raised.

The third item constitutes an essential difference to the spectral-domain method. In this method the electromagnetic field is expressed in terms of the unknown slot field components. Hence, raising the number of slots increases the number of unknowns. In our method, the complexity of the evaluation procedure is, however, not affected by the number of slots.

Numerically investigating the convergence of the series in (5) has shown that $F_{si} = f_i(t, s) f_i(p, s) b/d_i$ monotonically increases up to a maximum value which is achieved at s being the nearest integer to a certain s_m. The latter has been found from (5) by differentiation. It reads

$$s_m = \left[(p^2 + t^2)/2\right]^{1/2} d_i/b. \tag{7}$$

For $s > s_m$, F_{si} strongly decreases and can be neglected when s exceeds $s_m + \Delta s$. Δs depends on the ratio of the slot width to the waveguide height. This is analogous to the phenomenon of relative convergence discussed in [4]. For example, $\Delta s \approx 0.5$ for $d_i/b = 0.3$. The magnitude of Δs must be found numerically for every d_i/b.

The propagation constant is found by equating the determinant of the homogeneous system (4) to zero. As an example, numerical results for a microstrip with tuning septum are compared with published values taken from [5] (see Fig. 2). n_1 denotes the upper summation index in the series expansion of the potential functions (1). The agreement is excellent for larger widths of the septum, and it is somewhat poorer for small widths, which is, however, due to the truncation of the series used in [5].

The shielded microstrip treated in [6] is taken as a second example. In this case, our solution converges very fast and coincides with the results of [6] (see Fig. 3). Comparisons to published results for fin-lines with one or two slots also showed a good agreement. They will not be given here because we will still compare our approximate relations derived below to the literature.

III. Approximate Relations at Cutoff

Up to now, the computer time is very large. Moreover, one must be very careful in order not to overlook one or the other zero of the determinant. Both restrictions can be removed for all eigenmodes showing a cutoff frequency. Hence, the following analysis does not cover the fundamental mode of a microstrip line or the even mode of a double-slot fin-line. It is, however, valid for nearly all higher order modes of the general planar transmission line which do show a cutoff frequency. In particular, it is valid for all modes of the bilateral, unilateral, and antipodal fin-line. The first step is to replace the analysis by a calculation at the cutoff frequency of every mode. Then the HE-modes are reduced to pure TE-modes and the EH-modes to pure TM-modes. Equations (4) are then decoupled and can be solved separately. Equating their determinants to zero yields the cutoff frequencies. The propagation constants can be calculated from the cutoff frequencies by utilizing the concept of an equivalent dielectric constant k_e, which has been introduced in [7]. Our calculations have proven that the equivalent dielectric constant is nearly constant versus frequency as has been claimed [7] provided that the relative dielectric constant ϵ_r of the substrate material is only small.

The substrate material, which is often used, is RT-duroid with $\epsilon_r = 2.22$. In this case, k_e may be assumed to be constant. It can then be calculated from its definition as the squared ratio of the cutoff wavenumber for $\epsilon_r = 1$ to that obtained for the actual ϵ_r.

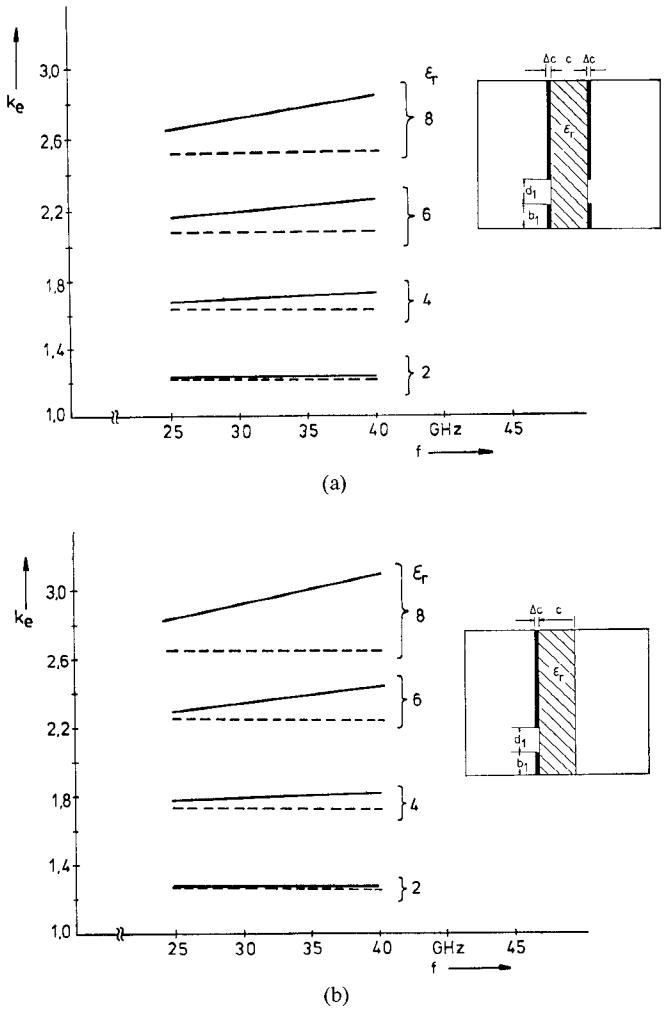

Fig. 4. Equivalent dielectric constant versus frequency (solid lines). (a) Bilateral, (b) unilateral fin-line. $a = 7.12$ mm, $b = a/2$, $c = 0.125$ mm, $\Delta c = 0.0175$ mm, $\epsilon_r = 2.22$. Dashed lines denote k_e at cutoff.

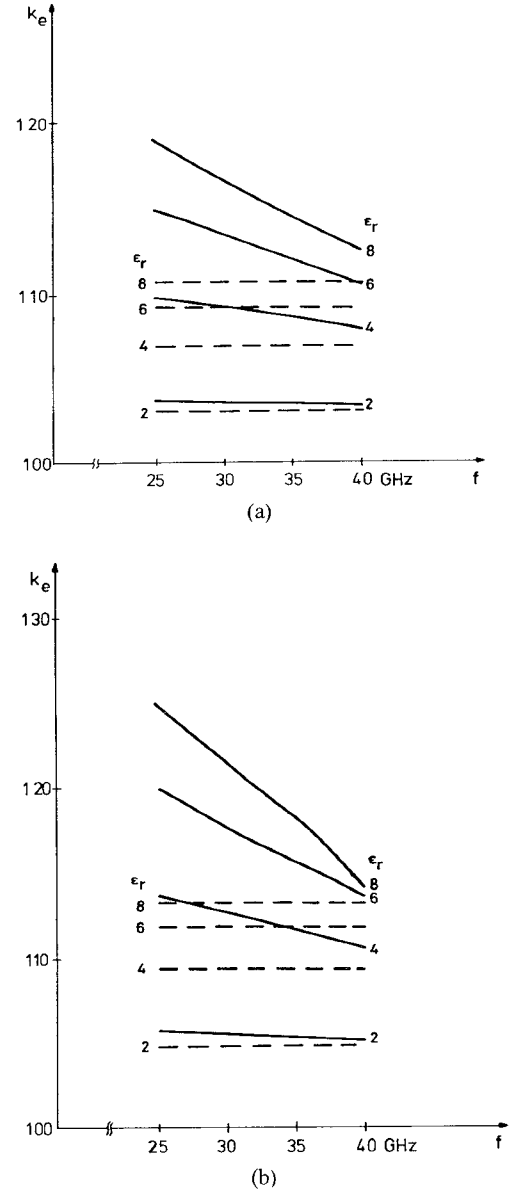

Fig. 5 Equivalent dielectric constant of the HE_{30}-mode versus frequency (solid lines). Parameters as in Fig. 4; dashed lines denote k_e at cutoff.

The concept of an equivalent dielectric constant is justified by this feature alone. Moreover, the numerical calculations show that this quantity is of large practical importance even for arbitrary permittivities, because it depends on frequency linearly. This is illustrated in Fig. 4(a) and (b), which show the equivalent dielectric constant of a unilateral and a bilateral fin-line with one slot. The solid lines have been computed from the dispersion relation

$$k_z^2 = k_e k^2 - k_c^2(\epsilon_r = 1) \tag{8}$$

by inserting numerically found values for k_z. It is obvious that k_e can be approximated at frequency f by

$$k_e(f) = k_e(f_c) + g\left(\epsilon_r^2 - k_e^2(f_c)\right)(k - k_c). \tag{9}$$

g is a constant which can be determined either experimentally or from the exact numerical solution at an arbitrary frequency.

The linear frequency dependence of the equivalent dielectric constant has recently been proven experimentally [8] and modeled empirically [8]. In order to illustrate the validity of (9), we have compared exact and approximate propagation constants in Table I. The agreement is good even at the upper band edge. The same statements are also valid for antipodal fin-lines. Furthermore, the straight-line approximation to $k_e(f)$ may also be applied to higher order modes. This is illustrated in Fig. 5 for the HE_{30}-mode.

TABLE I
COMPARISON BETWEEN EXACT AND APPROXIMATE PROPAGATION CONSTANTS OF FIN-LINES WITH ONE AND TWO SLOTS

		bilateral fin-line		unilateral fin-line	
d_2/b	f/GHz	25	40	25	40
0.0	$k_{z\,appr}$	0.520	0 884	0.519	0.890
	$k_{z\,ex}$	0 522	0 890	0.523	0.896
0 2	$k_{z\,appr}$	0.429	0.828	0.411	0.819
	$k_{z\,ex}$	0.430	0.831	0.413	0.823

WR-28 waveguide, $\epsilon_r = 2.22$, $d_1/b = 0.1 = b_1/b$, $b_2/b = 0.6$, $l_1 = l_2 = 3.4155$ mm, $c = 0.254$ mm, $\Delta c = 0.0175$ mm.

Although the quality of the approximation is poorer now, the influence on calculations should be small because these modes are normally below cutoff. Hence, the weight of the k_e-term in the dispersion relation is small.

Summarizing the results of this section we can state the following. The eigenmode analysis may be performed at cutoff and the dispersion relation thereafter approximated by using the concept of an equivalent dielectric constant. The computer time can thus be reduced by a factor of $1:N$, with N being the number of interesting frequencies. If the accuracy should be insufficient in a particular case, one can utilize the approximate propagation constants as initial values when looking for zeros in the coefficient determinant of (4).

IV. Relations Between Fundamental and Higher Order Modes

Up to now, the cutoff frequency of every wanted higher order eigenmode must still be calculated. This can be avoided by a second approximation which establishes a relation between all higher order modes and the fundamental mode for those transmission lines whose fundamental mode shows a cutoff frequency. Combining (4) with (A2)–(A3) at cutoff yields

$$f(t)=\sum_{p=0}^{\infty} X_p^{(1)}\cdot F_1(t,p),\quad \bar{f}(t)=\sum_{p=1}^{\infty} \bar{X}_p^{(1)}\cdot \bar{F}_1(t,p). \tag{10}$$

Furthermore

$$X_p^{(1)}=A_p\left(H_{1p}^{(1)}+H_p\cdot H_{2p}^{(1)}\right)$$
$$\bar{X}_p^{(1)}=\bar{A}_p\left(\bar{E}_{1p}^{(1)}-\bar{E}_p\cdot \bar{E}_{2p}^{(1)}\right)$$
$$H_p=\frac{G_p}{A_p},\quad \bar{E}_p=\frac{\bar{G}_p}{\bar{A}_p}. \tag{11}$$

Abbreviations H and $\bar{E}$ have been defined in Appendix II. Defining

$$g_t=\frac{(1+\epsilon_t)\cdot\Delta c}{\sum_{p=0}^{\infty}\frac{X_p^{(1)}}{X_t^{(1)}}\cdot F_1(t,p)}$$
$$\bar{g}_t=\frac{\Delta c}{\sum_{P=1}^{\infty}\frac{\bar{X}_p^{(1)}}{\bar{X}_t^{(1)}}\cdot \bar{F}_1(t,p)} \tag{12}$$

(10) can be rewritten

$$X_t^{(1)}=g_t f(t)^1/[(1+\epsilon_t)\Delta c],\quad \bar{X}_t^{(1)}=\bar{g}_t\bar{f}(t)^2/\Delta c. \tag{13}$$

These relations can be interpreted physically. For a single-slot fin-line with $d_1=b$ one finds from (5) and (6) $f_1(p_1,p_2)=1$ for $p_1=p_2=t>1$, $F_1(p,t)=\bar{F}_1(p,t)=0$ for $p\neq t$, and $F_1(0,0)=2$. Hence, $g_t=\bar{g}_t=\Delta c$ for arbitrary t. The fin-line is now reduced to a waveguide with dielectric slab loading. Its eigenvalues are found from the zeros of the coefficient determinants in (13). These relations are the characteristic equations for the case of a fin-line $d_1<b$, too. The problem then is to determine both g_t and $\bar{g}_t$. Their physical meaning can be derived from (12). (Note that this is an inherent advantage of the mode-matching method!) Now $g_t, \bar{g}_t \neq \Delta c$ because of the effect of the metal fins. As is also known from ridged waveguides, the fins lower the cutoff frequencies of the HE-modes but enhance those of the EH-modes. Hence, g_t must represent a capacitive and $\bar{g}_t$ an inductive effect.

TABLE II
Comparison Between Exact and Approximate Cutoff Wave Numbers of a Bilateral Fin-Line

m,n	k_c(exact)	k_c(approx.)	
1,0	0.252	-	HE-modes
1,1	0.879	-	
3,0	0.998	1.002	
5,1	2.041	2.039	
1,3	2.658	2.646	
1,1	1.279	-	EH-modes
2,1	1.923	1.925	
1,2	1.986	-	
3,1	2.044	2 050	
3,2	2.545	2 535	
5,1	2.907	2.913	

$d_1=0.56$ mm, $b_1=1.5$ mm, other parameters as in Table I.

In summary, g_t and $\bar{g}_t$ model the effect of the fringing fields near the fin-line slots. It has been found from the exact calculations that both quantities are nearly independent of the order m of the modes. (This is also supported by ridged waveguide calculations [9].) Moreover, one may assume that g_t and $\bar{g}_t$ do not depend on indices t or n, respectively, because the perturbation due to the fins appears in the x-direction. This latter assumption can, however, only be expected to be valid for either n,t even or n,t odd. The validity of these approximations has been thoroughly checked numerically. Quantitative results will be presented below.

Hence, $g_0\approx g_2\approx g_4\approx\cdots$, $g_1\approx g_3\approx g_5\approx\cdots$, $\bar{g}_1\approx\bar{g}_3\approx\bar{g}_5\approx\cdots$, and $\bar{g}_2\approx\bar{g}_4\approx\bar{g}_6\approx\cdots$ is valid. It is then possible to calculate the eigenvalues of the higher order modes from the eigenvalue of the lowest order mode. This will at first be shown for the bilateral fin-line. Let us assume m odd. The characteristic equation can then be derived from (11), (13), (A2), and (A3) to read

$$\cot(k_{xp}l)=k_{xp}g_q+\epsilon_r\cdot\frac{k_{xp}}{\bar{k}_{xp}}\tan(\bar{k}_{xp}\cdot c/2)\equiv B. \tag{14}$$

Here t has been changed in p. Furthermore, $q=0$ for p,n even and $q=1$ for p,n odd. (14) is used to determine g_0 and g_1, respectively, by inserting exactly calculated eigenvalues for the HE_{10}- and HE_{11}-mode, respectively. It can afterwards be solved for the higher eigenvalues by setting $(k_{xp}l)=(m_q\pi+\Delta q)$ where $m_q=(m-1)/2$. Then one arrives at $\cot(\Delta_q)=B$. This relation can iteratively be solved together with (14). The whole procedure will be explained in detail elsewhere [10]. It can also be applied to the EH-modes and to unilateral fin-line. Its validity is illustrated by a comparison to exact values, which is given in Table II. Finally, the propagation constants of various modes (H-type and E-type) calculated either exactly or

TABLE III
COMPARISON BETWEEN EXACT AND APPROXIMATE PROPAGATION CONSTANTS OF A BILATERAL FIN-LINE AT 30 GHz

type	order m n	k_z(exact) 1/mm	k_z(appr.1) 1/mm	k_z(appr.2) 1/mm
H	1 0	0.636	0.636	0.636
H	1 2	j1.673	j1.673	j1.672
H	5 0	j1.772	j1.772	j1.790
E	1 2	j1.881	j1.884	j1.884
E	3 2	j2.479	j2.468	j2.457
H	5 2	j2.550	j2.549	j2.514
H	7 0	j2.756	j2.753	j2.728
E	5 2	j3.215	j3.206	j3.191
H	7 2	j3.279	j3.277	j3.249

Parameters as in Table II. appr. 1 means with approximate dispersion relation only, appr. 2 means with approximate calculation of the higher-order modes additionally.

approximately are shown in Table III. Two approximations have been used: either a constant k_e or a constant k_e together with the approximation to the higher order modes just discussed. The accuracy obtained should be sufficient for most applications.

Using the approximations to the higher order modes, the computer time is reduced by a ratio $2:M$ with M the number of wanted eigenmodes. The total reduction in computer time is hence $2:NM$, which is equivalent to a reduction by about two orders of magnitude.

V. SIMPLIFICATIONS FOR OPEN STRUCTURES

It has been shown above that F_{st} in (5) can be neglected for $s > s_m$. For narrow slots with $d_t \ll b$, it is then sufficient to take only the first term for $s = 0$ or for $s = 1$, respectively, into account. Then

$$F_{1,2}(t,p) \simeq F'_{1,2}(t)\cdot F'_{1,2}(p). \tag{15}$$

Similar relations are valid for $F_2(t,p)$, $\bar{F}_1(t,p)$, and $\bar{F}_2(t,p)$. In the following, we will only describe the analysis for the first of relations (4). Taking the equation for subscript $t = q$, one can eliminate $X_p^{(1)}$ by calculating the difference

$$f(t) - f'(q) = \sum_{\substack{p=0 \\ p\neq q}}^{\infty} X_p^{(1)}\cdot F'_1(t,p) \tag{16}$$

with

$$f'(q) = f(q)\cdot\frac{F_1(t,q)}{F_1(q,q)} \tag{17}$$

and

$$F'_1(t,p) = F_1(t,p) - \frac{F_1(t,q)\cdot F_1(q,p)}{F_1(q,q)}. \tag{18}$$

The right-hand side of (18) cancels because of (15). Hence, inserting (A1) into (16) yields

$$\frac{A_t}{A_q} = \frac{k_{xq}\cdot\sin(k_{xq}l_1)\cdot(1+\epsilon_q)}{k_{xt}\cdot\sin(k_{xt}l_1)\cdot(1+\epsilon_t)}\cdot\frac{F_1(t,q)}{F_1(q,q)}. \tag{19}$$

The expansion coefficients A_t have thus been related to A_q, which is the only unknown in (19). They are now inserted into equation number 'q' of the system (4), which is the characteristic equation for the HE-modes or EH-modes, respectively.

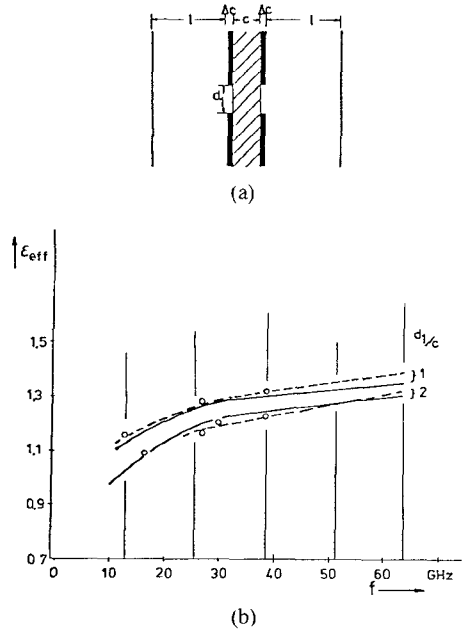

Fig. 6. (a) Cross section and (b) effective dielectric constant versus frequency of an open slot-line (solid lines). $l/c = 5$, $\Delta c = 0.0175$ mm, $\epsilon_r = 2.22$. 0 mean measurements; the dashed curves have been taken from [12].

TABLE IV
COMPARISON BETWEEN THIS THEORY AND [11] FOR $\epsilon_{eff} = (k_z^2/k^2)$ OF A UNILATERAL FIN-LINE AT 33 GHz

d_1	0.2	0.8	1.6 mm	$b_1 + d/2$
0.1	1.129 1.13	1.152 1.15	1.165 1.17	this theory Ref. 11
0.25 mm	1.061 1.06	1.066 1.06	1.074 1.07	this theory Ref. 11

Slot width d_1, height $b_1 + d/2$, $c = 0.125$ mm, other parameters as in Table I.

This technique is well suited for open structures. It can, however, also be used for a relatively small slot width. This is confirmed by a comparison between our approximate values for the propagation constant of the fundamental mode of a unilateral fin-line and values derived in [11] by using the spectral-domain method. The results given in Table IV show a good agreement. (In fact, the effective dielectric contant has been shown which is defined as the squared ratio between the propagation constant and the wavenumber.)

Finally, the effective dielectric constant of an open slot line (Fig. 6(a)) computed in this way is compared to results reported in [12] and to measurements in Fig. 6(b). The agreement is again good.

VI. CONCLUSIONS

A unified analysis of general planar transmission lines has been presented by using the mode-matching technique. The number of unknowns does not depend on the number

of slots or strips on the dielectric substrate if use is made of the metallization thickness being very small in almost all practical configurations. For all eigenmodes exhibiting a cutoff frequency, two assumptions are shown to be valid. The dispersion relations can easily be formulated by using the concept of an equivalent dielectric constant. All higher order modes can be derived from the fundamental mode. In addition, further simplifications to the characteristic equation are possible for small slot width and for open structures. By all of these means, the computer time is reduced by two orders of magnitude.

Appendix I

The various quantities appearing in (4) are

$$f(t) = A_t \cdot \sin(k_{xt} l_1) \cdot k_{xt} \cdot \Delta c \cdot (1 + \epsilon_t)$$
$$g(t) = G_t \cdot \sin(k_{xt} l_2) \cdot k_{xt} \cdot \Delta c \cdot (1 + \epsilon_t)$$
$$\bar{f}(t) = -\bar{A}_t \cdot \sin(k_{xt} l_1) \cdot k_{yt} \cdot \frac{k}{k_z \eta_0} \cdot \Delta c$$
$$\bar{g}(t) = \bar{G}_t \cdot \sin(k_{xt} l_2) \cdot k_{yt} \cdot \frac{k}{k_z \eta_0} \cdot \Delta c \qquad \text{(A1)}$$

$$X_p^{(1)} = A_p \cdot H_{1p}^{(1)} + G_p \cdot H_{2p}^{(1)} + \bar{A}_p \cdot E_{1p}^{(1)} - \bar{G}_p \cdot E_{2p}^{(1)}$$
$$X_p^{(2)} = A_p \cdot H_{1p}^{(2)} + G_p \cdot H_{2p}^{(2)} + \bar{A}_p \cdot E_{1p}^{(2)} - \bar{G}_p \cdot E_{2p}^{(2)}$$
$$\bar{X}_p^{(1)} = A_p \cdot \bar{H}_{1p}^{(1)} + G_p \cdot \bar{H}_{2p}^{(1)} + \bar{A}_p \cdot \bar{E}_{1p}^{(1)} - \bar{G}_p \cdot \bar{E}_{2p}^{(1)}$$
$$\bar{X}_p^{(2)} = A_p \cdot \bar{H}_{1p}^{(2)} + G_p \cdot \bar{H}_{2p}^{(2)} + \bar{A}_p \cdot \bar{E}_{1p}^{(2)} - \bar{G}_p \cdot \bar{E}_{2p}^{(2)} \qquad \text{(A2)}$$

with $\epsilon_t = 1$ for $t = 0$ and $\epsilon_t = 0$ otherwise. Furthermore

$$H_{1p}^{(i)} = F_{p1} + R_m \cdot R_p \cdot F_{p2} \quad H_{2p}^{(i)} = R_m \cdot R_p \cdot F_{p3}$$
$$E_{1p}^{(i)} = \left(L_m \cdot R_m \cdot k_p / \bar{k}_{xp}\right) \cdot F_{p2}$$
$$E_{2p}^{(i)} = \left(L_m \cdot R_m \cdot k_p / \bar{k}_{xp}\right) \cdot F_{p3}$$
$$\bar{H}_{1p}^{(i)} = \frac{1}{\eta_0^2} L_m \cdot R_m \cdot R_p \cdot F_{p2} \quad \bar{H}_{2p}^{(i)} = \frac{1}{\eta_0^2} L_m \cdot R_m \cdot R_p \cdot F_{p3}$$
$$\bar{E}_{1p}^{(i)} = \frac{k_{xp}}{k_p} F_{p1} + \left(\frac{1}{\eta_0^2} L_m^2 \cdot R_m^2 \cdot \frac{k_p}{\bar{k}_{xp}} + \frac{\epsilon_r \cdot \bar{k}_{xp}}{R_m k_p} \right) \cdot F_{p2}$$
$$\bar{E}_{2p}^{(i)} = \left(\frac{1}{\eta_0^2} L_m^2 \cdot R_m \cdot \frac{k_p}{\bar{k}_{xp}} + \frac{\epsilon_r \cdot \bar{k}_{xp}}{R_p k_p} \right) \cdot F_{p3} \qquad \text{(A3)}$$
$$\frac{k_{xp}}{\bar{k}_{xp}} = R_p \quad \frac{\bar{K}_{cmn}^2}{K_{cmn}^2} = R_m \quad \left(1 - \frac{1}{R_m}\right) = L_m$$
$$\frac{k_{yp} \cdot k_z \cdot \eta_0}{k} = k_p$$
$$F_{p1} = \cos(k_{xp} l_i) \quad F_{p2} = \sin(k_{xp} l_i) \cdot \cot(\bar{k}_{xp} c)$$
$$F_{p3} = \sin(k_{xp} l_s) / \sin(\bar{k}_{xp} c) \qquad \text{(A4)}$$

with $s = 1$ for $i = 2$ and $s = 2$ for $i = 1$.

Appendix II

Defining $H_p = G_p / A_p$ and $\bar{E}_p = \bar{G}_p / \bar{A}_p$, one finds from matching the tangential field components at the interfaces of the cross section (Fig. 1) $H_p = -1$, $\bar{E}_p = 1$ for the odd and $H_p = 1$, $\bar{E}_p = -1$ for the even modes of the bilateral fin-line. For the unilateral fin-line, one has

$$H_p = \frac{-H_{1p}^{(2)}}{H_{2p}^{(2)} - \left(g(p)/G_p\right)} \simeq \frac{-H_{1p}^{(2)}}{H_{2p}^{(2)}}$$
$$\bar{E}_p = \frac{-E_{1p}^{(2)}}{\bar{E}_{2p}^{(2)} - \left(\bar{g}(p)/\bar{G}_p\right)} \simeq \frac{-E_{1p}^{(2)}}{\bar{E}_{2p}^{(2)}} \qquad \text{(A5)}$$

because $\Delta c / a \ll 1$ and for the antipodal fin-line $H_p = (-1)^{p+1}$, $\bar{E}_p = (-1)^p$.

References

[1] T. Itoh, "Generalized spectral-domain method for multiconductor printed lines and its application to tunable suspended microstrips," *IEEE Trans. Microwave Theory Tech.*, vol. MTT-26, pp. 983–987, Dec. 1978.

[2] L. Schmidt and T. Itoh, "Spectral-domain analysis of dominant and higher order modes in fin-lines," *IEEE Trans. Microwave Theory Tech.*, vol. MTT-28, pp. 981–985, Sept. 1980.

[3] A. Beyer and I. Wolff, "A solution of the earthed fin-line with finite metallization thickness," in *IEEE MTT Symp. Dig.*, 1980, pp. 255–257.

[4] R. Mittra, T. Itoh, and T. S. Li, "Analytical and numerical studies of the relative convergence phenomenon arising in the solution of an integral equation by the moment method," *IEEE Trans. Microwave Theory Tech.*, vol. MTT-20, pp. 96–104, Feb. 1972.

[5] T. Itoh, "Spectral-domain immittance approach for dispersion characteristics of shielded microstrips with tuning septums," in *Proc. 9th Euro. Microwave Conf.*, (Brighton), 1979, pp. 435–439.

[6] T. Itoh and R. Mittra, "A technique for computing dispersion characteristics of shielded microstrip lines," *IEEE Trans. Microwave Theory Tech.*, vol. MTT-22, pp. 896–898, Oct. 1974.

[7] P. J. Meier, "Integrated fin-line millimeter components," *IEEE Trans. Microwave Theory Tech.*, vol. MTT-22, 1974, pp. 1209–1216, 1974.

[8] A. K. Sharma and W. J. R. Hoefer, "Empirical analytical expressions for fin-line design," in *IEEE MTT Symp. Dig.*, 1981, pp. 102–104.

[9] S. Hopfer, "The design of ridged waveguide," *IRE Trans. Microwave Theory Tech.*, vol. MTT-3, pp. 20–29, Oct. 1955.

[10] A. M. K. Saad and K. Schünemann, "Closed-form approximations for fin-line eigenmodes," accepted for publication in *Proc. Inst. Elec. Eng.*, part H(MOA), 1982.

[11] L. P. Schmidt, T. Itoh, and H. Hofmann, "Characteristics of unilateral fin-line structure with arbitrarily located slots," in *IEEE MTT Symp. Dig.*, 1980, pp. 255–257.

[12] A. M. A. El-Sherbiny, "Exact analysis of shielded microstrip lines and bilateral fin-lines," *IEEE Trans. Microwave Theory Tech.*, vol. MTT-29, pp. 669–675, July 1981.

Abdel Megid Kamal Saad was born in Behera, Egypt, on September 3, 1943. He received the B.S. degree in electrical engineering in 1966, and the M.S. degree in 1973, both from Ain-Shams University in Cairo.

From 1968 to 1971 he was in the army service. Since 1974 he has been working at the Institut für Hochfrequenztechnik of the Technische Universität Braunschweig, Braunschweig, West Germany, where, in 1982, he received the Ph.D. degree. His current research interest is in the field of microwave integrated-circuit techniques in the millimeter-wave region.

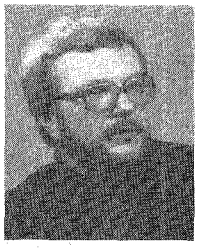

Klaus Schünemann (M'77) was born in Braunschweig, West Germany, on June 17, 1939. He received the master's degree in electrical engineering (Dipl.-Ing.) and his doctorate of engineering (Dr.-Ing.) from the Technische Universität Braunschweig, West Germany, in 1965 and 1970, respectively.

From 1965 to 1970 he was a Research Assistant at the Department of Electrical Engineering of the Technical University Braunschweig (Institut für Hochfrequenztechnik), where he was engaged in investigations on frequency multiplication and on diode modelling for switching applications. From 1970 to 1971 he worked for Valvo GmbH of Hamburg, West Germany, in the area of high-power, high-stable, solid-state oscillators. Since 1972, he has been back with the Institut für Hochfrequenztechnik (Electrical Engineering Department of the Technical University Braunschweig), where he has been involved with investigations on high-speed modulators for PCM communication systems and on amplification and noise in solid-state oscillators. He is now a Professor in the Electrical Engineering Department and his current research interests are primarily concerned with new technologies for microwave integrated circuits, such as fin-line and waveguide-below-cutoff techniques, and with transport phenomena in submicron structures.

Hybrid Fin-Line Matching Structures

HADIA EL HENNAWY, STUDENT MEMBER, IEEE, AND KLAUS SCHÜNEMANN, MEMBER, IEEE

Abstract—**Two transitions between unilateral and bilateral fin-line mounted back to back show unique features for impedance transformation. The series reactances of the equivalent T-circuit are theoretically shown to be capacitive. This is exploited by designing a broad-band switch with two p-i-n diodes. Its isolation is about 20 dB throughout the *Ka*-band.**

I. Introduction

THE BASIC building blocks of fin-line circuits are various discontinuities in the slot width. Impedance transformation is usually performed with either one or two steps in the slot width [1]. With two cascaded steps one can generate either a notch or a strip. Almost all known components are realized in this way. These structures can be analyzed by combining an eigenmode with a modal analysis [2]. The procedure has been carried through in [1]. We will apply this method here to new configurations.

The structures for impedance transformation to be described show both electrical and practical advantages over the known ones. Their slot patterns are sketched in Fig. 1. These structures consist of two cascaded transitions between unilateral and bilateral fin-lines of equal slot widths. The slot may be located either symmetrically or unsymmetrically with respect to the waveguide axis. A large range of impedances can be generated by varying two geometrical parameters: the common slot width $2s$ and the length $2l$ of the middle section. Such a line section can therefore be used in either of two ways: as an impedance transformer or as a semiconductor device mount. In the latter application, the circuit patterns show a practical advantage over conventional ones. While the circuit at the front side which contains the semiconductor devices is protected against damage, one can conveniently alter the transforming section on the back side of the substrate in order to optimize performance. In addition, there are, however, even electrical advantages over the usual notch and strip patterns, which will be derived in the following.

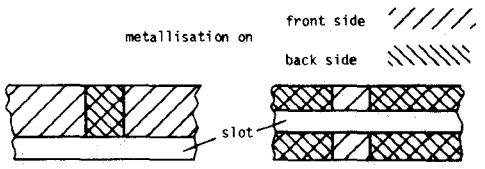

Fig. 1. Slot patterns of transitions between unilateral and bilateral fin-lines.

II. Modal Analysis

In order to analyze the structures shown in Fig. 1, one must know both the propagation constants and the field distributions of the hybrid eigenmodes of unilateral and bilateral fin-lines. The problem has been solved by a number of authors. We have adopted the spectral-domain technique presented, e.g., in [3] and modified it to determine the eigenmodes of both unilateral and bilateral fin-line in a unified form. The unilateral fin-line case is treated in Appendix I, while the results for the bilateral fin-line will be presented elsewhere [4]. The notation is the same for both cases. The key to an efficient eigenmode evaluation is a suitable choice of the system of basis functions into which the slot fields must be expanded. This has been discussed in [3]. We have used a fifth-order polynomial modified by a square-root term in order to take the edge condition correctly into account. Thus it was possible to calculate up to 30 eigenmodes with sufficient accuracy.

The modal analysis for computing the characteristics of an abrupt transition between a bilateral and a unilateral fin-line shall be briefly described (compare also to [5]). As

Manuscript received March 10, 1982; revised June 4, 1982.

K. Schünemann is with the Institut für Hochfrequenztechnik, Technische Universität Braunschweig, D-3300 Braunschweig, West Germany.

H. El Hennawy is with Ain Shams University, Cairo, Egypt.

0018-9480/82/1200-2132$00.75 ©1982 IEEE